LAWRENCE
LIVERMORE
NATIONAL
LABORATORY

LLNL-JRNL-755419

U-Pb constraints on pulsed eruption of the Deccan Traps across the end-Cretaceous mass extinction

B. Schoene, M. P. Eddy, K. M. Samperton, C. B. Keller, G. Keller, T. Adatte, S. F. R. Khadri

July 27, 2018

Science

U-Pb constraints on pulsed eruption of the Deccan Traps across the end-Cretaceous mass extinction

Blair Schoene[1*], Michael P. Eddy[1], Kyle M. Samperton[2], C. Brenhin Keller[3], Gerta Keller[1], Thierry Adatte[4], Syed F.R. Khadri[5]

1. Department of Geosciences, Princeton University, Princeton, NJ, USA; *corresponding author: bschoene@princeton.edu
2. Nuclear and Chemical Sciences Division, Lawrence Livermore National Laboratory, Livermore, CA, USA
3. Berkeley Geochronology Center, Berkeley, CA, USA
4. ISTE, Institut des Sciences de la Terre, Université de Lausanne, GEOPOLIS, Lausanne, Switzerland
5. Department of Geology, Amravati University, Amravati, India

One sentence summary:

The Deccan Traps erupted as four major pulses spanning the K-Pg mass extinction.

Abstract:

Temporal correlation between some continental flood basalt eruptions and mass extinctions has been proposed to indicate causality, with eruptive volatile release driving environmental degradation and extinction. We test this model for the Deccan Traps flood basalt province, which, along with the Chicxulub bolide impact, is implicated in the Cretaceous-Paleogene (K-Pg) extinction ca. 66 million years ago. We estimate Deccan eruption rates with U-Pb zircon geochronology, and resolve four high-volume eruptive periods. Maximum eruption rates are observed before and after the K-Pg extinction, with one such pulse initiating tens of thousands of years prior to both the bolide impact and extinction. These findings support extinction models that incorporate both catastrophic events as drivers of environmental deterioration associated with the K-Pg extinction and its aftermath.

Main Text:

Continental flood basalt provinces are characterized by eruption of >1 million km^3 of basalt over <1 million years (*1, 2*), representing the largest volcanic events on Earth. Four of the five most severe Phanerozoic mass extinctions (~541 million years ago (Ma) to the present) coincided with emplacement of one of these provinces (*3*). While the temporal link between flood basalts and extinctions is well-established, the mechanisms by which eruptions drive extinction are poorly understood (*4*). Two models of environmental change from volcanic activity relate to eruptive volatile emissions (*1, 4*). The first is volcanogenic CO_2 release, with associated global warming, ocean acidification, and carbon cycle disruption. The second is SO_2 injection into the stratosphere and its conversion to sulfate aerosols, causing global cooling, acid rain and ecosystem poisoning (*5*). The predicted timescales of these perturbations contrast sharply. The emission of SO_2 from a single eruption would produce years of cooling, whereas accumulated greenhouse warming from CO_2 can be sustained for many thousands to tens of thousands of years (kyr). Testing the effects of this interplay on ecosystems thus requires precisely-calibrated volcanic eruption rates that can be correlated to high-resolution climate proxy and biostratigraphic data.

We applied U-Pb zircon geochronology to construct a precise temporal record of eruption within the Deccan Traps volcanic province, India (Fig. 1). The province is temporally correlated to the K-Pg mass extinction, in which roughly three quarters of life on Earth was eradicated, including non-avian dinosaurs (*6*). Previous attempts to constrain eruption rates were limited by poor stratigraphic coverage and/or high analytical uncertainties (*7-12*). We used U-Pb geochronology by isotope dilution–thermal ionization mass spectrometry (ID-TIMS; *ref.13*), which provides analytical uncertainties as low as 40 kyr (±2σ) for individual dated zircons. Our sampling covers the nine major Deccan formations in the Western Ghats, where the most voluminous (>90% total volume) and complete Deccan exposures are preserved (*14-17;* Fig. 1). We sampled both coarse-grained basalts and sedimentary beds between basalt flows that infrequently contain zircon-bearing volcanic ash (*11*; Fig. S1). These beds, locally termed "redboles", range from oxidized volcaniclastic material with visible lithic fragments and phenocrysts, to paleosol-type horizons produced by *in situ* weathering of flow tops (*18, 19*). Of 141 sampled redboles and coarse-grained basalts (Figs. 1 and S1-S2), 23 redboles and one basalt sample yielded sufficient zircon (≥5 crystals) to estimate an eruption age, including four distinct bole horizons and one basalt previously presented by Schoene et al. (*11*). Pristine volcanic crystal morphology indicates minimal transportation/reworking of zircon in a sedimentary environment. Consequently, we inferred that this volcaniclastic, zircon-bearing material was incorporated into redboles as air fall tuff, consistent with some redboles containing a high-SiO_2 (non-basaltic) component (*19*), and that these zircons provide a robust means for dating Deccan eruptive stratigraphy.

To estimate the eruption date and associated uncertainty for each sample, we developed an approach using Bayesian statistics to account for the probability distribution of zircon dates and their analytical uncertainties (*20;* Fig. S6). While we considered alternative data interpretations (*13*), they do not affect the conclusions of this study. Twenty-one of 24 dated horizons are from five stratigraphic sections along prominent roads in the Western Ghats, providing complete coverage of the upper four Deccan formations (Fig. 1; Fig. S1-S2). The remaining three samples span the lower five Deccan formations, where redboles are rare and less likely to contain zircon.

When compiled into a composite stratigraphic section (Fig. 1), almost all samples follow anticipated "younging-up" temporal order based on the independently-defined regional stratigraphy (*14-17;* Fig. S2, S7). The exception is the Katraj Ghat south of Pune city, where two samples from what was mapped as upper Poladpur Formation (Fm) are ca. 100 kyr younger than samples near the Poladpur-Ambenali contact in other sections. To resolve this discrepancy, we placed the Poladpur-Ambenali contact in the Katraj Ghat section as ~100 m lower than previously mapped. This simple adjustment does not violate geochemical or geological observations in the stratigraphy, as the Poladpur-Ambenali contact is geochemically transitional in published datasets (*14*).

Furthermore, our placement of the contact is consistent with geochemical studies of the nearby Sinhagad Fort section suggesting the Poladpur Fm is relatively thin just south of Pune (*14*).

To further refine the composite stratigraphic age model, we employed a Bayesian Markov Chain Monte Carlo (MCMC) model in which stratigraphic superposition is imposed on U-Pb zircon dates (*13, 21*; Fig. 1). The result is a deposition age estimate for each dated horizon, incorporating dates from all beds above and below each sample to produce an internally consistent age model (Fig. 1). Accuracy of refined age estimates depends solely on sample placement in proper stratigraphic order, and is independent of samples' exact stratigraphic heights.

To calculate volumetric eruption rates through the Deccan Traps, we adopted the volume model of Richards et al. (*22*), in which units of the Wai subgroup (i.e., the Poladpur, Ambenali and Mahabaleshwar Fms) were interpreted as more voluminous than is apparent from their proportionate thickness in the Western Ghats. While this assertion carries nontrivial uncertainties, we believe it is justified given correlation of these formations to basalt flows on the province's periphery, including massive flows that traveled ~1000 km to India's eastern shore (*23, 24*). While different volume models produce changes in the *magnitude* of calculated eruption rates, the *timing* of peak eruption rates is unaffected by either the volume model or the interpretation approach of the zircon data (*13*; Fig. S8, S9). Additional uncertainty relates to the unconstrained mass and age of Deccan basalt that is currently submerged and inaccessible off India's western shore. We consider this uncertainty to be intractable as current volume models cannot account for this mass component of the province. Consequently, all eruption rates are likely minimum estimates, although we also cannot assess whether the offshore component erupted during the same time intervals as that of the Western Ghats.

We converted our age model into a probabilistic estimate of volumetric flux of basaltic lava using outputs from the MCMC algorithm (Fig. 2). Our results showed that the Deccan Traps erupted in four high-volume events, lasting ≤100 kyr each, separated by periods of relative volcanic quiescence. The first event corresponded to the eruption of the lowermost seven formations from ~66.3–66.15 Ma; the second to the Poladpur Fm from ~66.1–66.0 Ma; the third to the Ambenali Fm from ~65.9–65.8 Ma; and the fourth and final to the uppermost Mahabaleshwar Fm, from ~65.6–66.5 Ma.

Our Deccan eruption model (Fig. 2) constrains the volcanic tempo with high resolution, providing a means to correlate eruption records with biostratigraphic and climate proxy data across the K-Pg extinction. Our model places the second pulse of Deccan volcanism (Poladpur Fm, 66.1–66.0 Ma) as slightly predating a published U-Pb zircon date for the K-Pg boundary (KPB), defined as the Ir-anomaly and associated fallout from the Chicxulub impact, within the Denver Basin, Colorado (*25*). For consistency, we applied the Bayesian approach to that dataset (*25*) to estimate a date of 66.016±0.050 Ma for the KPB (95% C.I., internal uncertainties only, *13*). Comparison of our data with recently published $^{40}Ar/^{39}Ar$ geochronology from the Deccan Traps and the Chicxulub impact (*12, 26*) is currently not possible at the necessary level of precision given systematic bias between the two dating methods, primarily related to uncertainty in ages of $^{40}Ar/^{39}Ar$ fluence monitors and the values of the ^{40}K decay constant and physical constants (*13*). Assuming that the Chicxulub impact coincides exactly with the main phase of extinction, the MCMC model outputs from our Deccan data demonstrate a ~90% probability that the Poladpur Fm. eruption pulse began tens of kyr before the K-Pg mass extinction event.

The K-Pg extinction preserves the only known mass extinction that coincides with both a large igneous province and a bolide impact. As such, several hypotheses have been forwarded in which the impact triggered or modulated volcanic eruptions. While the most recent iteration of this hypothesis concedes initiation of Deccan eruptions several hundred kyr before the impact, it proposes impact-induced seismicity increased eruption rates in the Deccan Traps and at mid-ocean ridges through evacuation of pre-existing magma chambers in the upper mantle/lower crust (*12, 22, 27*). It is unlikely that our Deccan eruptive history is consistent with this model, given the high probability that the Poladpur pulse began before the impact by tens of kyr, followed by an eruption hiatus of ≤100 kyr after the impact.

Estimates for the entire volcanic flux on Earth today are 3-4 km^3/yr (*28*), indicating on average a doubling in global volcanic activity for ≤100 kyr during each of the four high-volume Deccan eruptive events, but requiring periods of >5-10 times the global average. In fact, groups of flows within the Poladpur and Mahabaleshwar Fms, each potentially comprising >50,000 km^3, lack secular evolution in paleomagnetic poles, suggesting eruption over decades to centuries (*29*). Such high eruption rates of >1000 km^3/year are permitted by our U-Pb geochronology, requiring hiatuses of 100s to 1000s of years within our resolved pulses so as not to exceed total volume estimates. In addition to being consistent with brief but extreme eruption rates, our data demonstrate that the Deccan Traps erupted in pulses with durations of ca. 100 kyr, providing insight into tempos of melt production and/or transport in the upper mantle and lower crust (*30, 31*).

Our eruption rate model is a first step towards robustly evaluating environmental impacts associated with Deccan volcanism. The most commonly cited contributors to environmental change associated with flood basalts are CO_2 (warming), SO_2 (cooling upon conversion to sulfate aerosols), and chemical weathering of fresh basaltic material (cooling via CO_2 drawdown). For single continental flood basalt flows that erupt over a few decades, volcanic SO_2 has been modeled to drive cooling of 5-10 ˚C for the duration of the eruption (*5*), after which acid rain rapidly removes sulfur compounds from the atmosphere. For persistent cooling over many kyr, therefore, hiatuses of only several decades between eruptions are required (*5*).

In contrast to SO_2, the timescale of CO_2 removal from the ocean-atmosphere system is slow, ~1, ~10, and ~100 kyr, for mixing into the deep ocean, reaction with sediments, and removal by silicate weathering, respectively (*32, 33*). As a result, while climate effects *during* an eruptive event may be dominated by cooling associated with elevated sulfate aerosols, on intermediate timescales *between* eruptive events, accumulation of volcanic CO_2 emissions can lead to net warming. On timescales of 100s of kyr to >1 Myr, weathering of fresh basalt has been modeled to result in net CO_2

drawdown and cooling, especially if the basalt is at low latitudes, as were the Deccan Traps (*34*).

As an initial attempt to correlate our eruptive history with paleoenvironmental data, we use two proxy records across the K-Pg transition (Fig. 2B). Benthic foraminifera $\delta^{18}O$ compositions indicate ~2-4 ˚C of deep ocean warming over ~150 kyr, beginning at the C30n-C29r magnetic reversal ~66.3 Ma, followed by cooling over ~150 kyr prior to the KPB (*35*-*37*). It has also been argued on the basis of $\delta^{18}O$ data from Elles, Tunisia, that renewed warming began tens of thousands of years before the KPB (*38;* Fig. S11).

Initial warming at ~66.3 Ma and a coeval increase in carbonate dissolution have been interpreted as resulting from volcanogenic CO_2 build-up and consequent ocean acidification (*35*), which our geochronology shows occurred during the initial pulse of Deccan eruptions. Warming curtailed towards the end of the first pulse, and cooling began before and continued through the initiation of the Poladpur Fm eruptions (Fig. 2). The extrusion of the voluminous Poladpur Fm may have resulted in short periods of SO_2-driven cooling that could have continued to promote the overall cooling trend, but cooling for tens of kyr due to SO_2 emissions is difficult to sustain given the predicted short residence time of sulfate aerosol (*1, 5*). Alternatively, an increase in surface area of exposed basalt associated with eruption of the Poladpur is possible given current Deccan stratigraphic area/volume models (*22*), resulting in enhanced basalt weathering, CO_2 drawdown, and continued global cooling in the tens of kyr before the extinction. If periods of cooling did result from sulfate aerosols during the Poladpur eruptions, the short intervals of temperature decrease could have slowed silicate weathering and associated CO_2 drawdown, thus permitting CO_2 build-up in the atmosphere that would be manifest between punctuated eruptions within the Poladpur Fm (*39*).

Testing whether basalt weathering was important leading up to the KPB is aided through study of the Os isotope system in marine carbonates because the ocean residence time of Os is short and basaltic $^{187}Os/^{188}Os$ is low (0.1; *ref. 10*) relative to late Mesozoic seawater (0.6; *ref. 40*). Published Os isotopic data from marine carbonates (*40*) show a dramatic decrease towards mantle values beginning at the onset of Deccan volcanism (Fig. 2B). A second downturn in $^{187}Os/^{188}Os$, beginning tens of kyr prior to the KPB, has been interpreted as a downward redistribution of extraterrestrial Os derived from the Chicxulub impactor (*40, 41*). However, this decrease is synchronous with the Poladpur eruption pulse, and is thus also consistent with increased weathering of a more extensive Deccan basalt pile.

Post-extinction and post-Chicxulub benthic foraminifera $\delta^{18}O$ and carbonate Os isotopic records do not covary with the Deccan eruption record. However, the Os record does not recover to the pre-Deccan $^{187}Os/^{188}Os$ value either, perhaps indicating that a steady state was reached between basalt production and weathering despite continued eruptions. Regardless, the starkly different responses of O and Os isotope records during the post-extinction recovery requires models that explicitly incorporate the effects of continued Deccan eruptions, the Chicxulub impact, and biotic effects on the carbon cycle in a world with devastated ecosystems.

While the initiation of a massive eruptive pulse shortly before the Chicxulub impact and mass extinction supports a Deccan contribution to ecosystem collapse, much remains to be discovered as to how flood basalt magmatism contributes to mass extinctions. U-Pb geochronology has shown that, similar to the K-Pg extinction, the end-Permian (~252 Ma) and end-Triassic (~201 Ma) mass extinctions occurred on short timescales (< tens of kyr), hundreds of kyr after the onsets of the Siberian Traps and Central Atlantic Magmatic Province flood basalt provinces, respectively (*42-44*). The eruptions and associated intrusive magmatism are presumed to have driven rapid extinction despite this time lag and the absence of bolide impacts. This lag between the onset of magmatism and extinction may be a result of highly nonlinear rates of magmatism as documented here for the Deccan Traps. Continuing to study other flood basalt provinces will clarify the importance of eruptive and intrusive tempo in driving ecosystem collapse and extinction. Such an understanding of biosphere sensitivity and threshold processes to climate change is as relevant today as during these catastrophic events in Earth history.

References Cited

1. S. Self, A. Schmidt, T. A. Mather, Emplacement characteristics, time scales, and volcanic gas release rates of continental flood basalt eruptions on Earth. *Geological Society of America Special Papers* **505**, (2014).

2. S. E. Bryan, I. U. Peate, D. W. Peate, S. Self, D. A. Jerram, M. R. Mawby, J. G. Marsh, J. A. Miller, The largest volcanic eruptions on Earth. *Earth-Science Reviews* **102**, 207 (2010).

3. V. E. Courtillot, P. R. Renne, On the ages of flood basalt events. *Comptes Rendus Geoscience* **335**, 113 (2003).

4. D. P. G. Bond, P. B. Wignall, Large igneous provinces and mass extinctions: An update. *Geological Society of America Special Papers* **505**, 29 (2014).

5. A. Schmidt, R. A. Skeffington, T. Thordarson, S. Self, P. M. Forster, A. Rap, A. Ridgwell, D. Fowler, M. Wilson, G. W. Mann, Selective environmental stress from sulphur emitted by continental flood basalt eruptions. *Nature Geoscience* **9**, 77 (2016).

6. J. J. Sepkoski, in *Global events and event stratigraphy in the Phanerozoic*. (Springer, 1996), pp. 35-51.

7. R. A. Duncan, D. G. Pyle, Rapid eruption of the Deccan flood basalts at the Cretaceous/Tertiary boundary. *Nature* **333**, 841 (06/30/print, 1988).

8. V. Courtillot, G. Feraud, H. Maluski, D. Vandamme, M. G. Moreau, J. Besse, Deccan flood basalts and the Cretaceous/Tertiary boundary. *Nature* **333**, 843 (1988).

9. A. Chenet, X. Quidelleur, F. Fluteau, V. Courtillot, S. Bajpai, 40K–40Ar dating of the Main Deccan large igneous province: Further evidence of KTB age and short duration. *Earth and Planetary Science Letters* **263**, 1 (2007).

10. C. Allegre, J. Birck, F. Capmas, V. Courtillot, Age of the Deccan traps using 187 Re–187 Os systematics. *Earth and Planetary Science Letters* **170**, 197 (1999).

11. B. Schoene, K. M. Samperton, M. P. Eddy, G. Keller, T. Adatte, S. A. Bowring, S. F. Khadri, B. Gertsch, U-Pb geochronology of the Deccan Traps and relation to the end-Cretaceous mass extinction. *Science* **347**, 182 (2015).

12. P. R. Renne, C. J. Sprain, M. A. Richards, S. Self, L. Vanderkluysen, K. Pande, State shift in Deccan volcanism at the Cretaceous-Paleogene boundary, possibly induced by impact. *Science* **350**, 76 (2015).

13. Materials and methods are available as supplementary materials on Science Online.

14. J. E. Beane, C. A. Turner, P. R. Hooper, K. V. Subbarao, J. N. Walsh, Stratigraphy, composition and form of the Deccan Basalts, Western Ghats, India. *Bulletin of Volcanology* **48**, 61 (1986).

15. A. E. Jay, M. Widdowson, Stratigraphy, structure and volcanology of the SE Deccan continental flood basalt province: implications for eruptive extent and volumes. *Journal of the Geological Society* **165**, 177 (2008).

16. S. Khadri, K. Subbarao, P. Hooper, J. Walsh, Stratigraphy of Thakurvadi formation, western Deccan basalt province, India. *Deccan flood basalts. Geol Soc Ind Mem* **10**, 281 (1988).

17. C. W. Devey, P. C. Lightfoot, Volcanological and tectonic control of stratigraphy and structure in the western Deccan Traps. *Bulletin of Volcanology* **48**, 195 (1986).

18. M. Widdowson, J. N. Walsh, K. V. Subbarao, The geochemistry of Indian bole horizons: palaeoenvironmental implications of Deccan intravolcanic palaeosurfaces. *Geological Society, London, Special Publications* **120**, 269 (1997).

19. P. Ghosh, M. R. G. Sayeed, R. Islam, S. M. Hundekari, Inter-basaltic clay (bole bed) horizons from Deccan traps of India: Implications for palaeo-weathering and palaeo-climate during Deccan volcanism. *Palaeogeography, Palaeoclimatology, Palaeoecology* **242**, 90 (2006).

20. C. B. Keller, B. Schoene, K. M. Samperton, A stochastic sampling approach to zircon eruption age interpretation. *Geochemical Perspectives Letters* **8**, 31 (2018).

21. C. E. Buck, C. D. Litton, A. F. Smith, Calibration of radiocarbon results pertaining to related archaeological events. *J Archaeol Sci* **19**, 497 (1992).

22. M. A. Richards, W. Alvarez, S. Self, L. Karlstrom, P. R. Renne, M. Manga, C. J. Sprain, J. Smit, L. Vanderkluysen, S. A. Gibson, Triggering of the largest Deccan eruptions by the Chicxulub impact. *Geological Society of America Bulletin* **127**, 1507 (2015).

23. K. B. Knight, P. R. Renne, A. Halkett, N. White, 40Ar/39Ar dating of the Rajahmundry Traps, Eastern India and their relationship to the Deccan Traps. *Earth and Planetary Science Letters* **208**, 85 (2003).

24. S. Self, A. E. Jay, M. Widdowson, L. P. Keszthelyi, Correlation of the Deccan and Rajahmundry Trap lavas: Are these the longest and largest lava flows on Earth? *Journal of Volcanology and Geothermal Research* **172**, 3 (2008).

25. W. C. Clyde, J. Ramezani, K. R. Johnson, S. A. Bowring, M. M. Jones, Direct high-precision U–Pb geochronology of the end-Cretaceous extinction and calibration of Paleocene astronomical timescales. *Earth and Planetary Science Letters* **452**, 272 (2016).

26. P. R. Renne, A. L. Deino, F. J. Hilgen, K. F. Kuiper, D. F. Mark, W. S. Mitchell, 3rd, L. E. Morgan, R. Mundil, J. Smit, Time scales of critical events around the Cretaceous-Paleogene boundary. *Science* **339**, 684 (2013).

27. J. S. Byrnes, L. Karlstrom, Anomalous K-Pg–aged seafloor attributed to impact-induced mid-ocean ridge magmatism. *Science advances* **4**, eaao2994 (2018).

28. J. A. Crisp, Rates of magma emplacement and volcanic output. *Journal of Volcanology and Geothermal Research* **20**, 177 (1984).

29. A.-L. Chenet, F. Fluteau, V. Courtillot, M. Gérard, K. V. Subbarao, Determination of rapid Deccan eruptions across the Cretaceous-Tertiary boundary using paleomagnetic secular variation: Results from a 1200-m-thick section in the Mahabaleshwar escarpment. *Journal of Geophysical Research* **113**, (2008).

30. L. Karlstrom, M. Richards, On the evolution of large ultramafic magma chambers and timescales for flood basalt eruptions. *Journal of Geophysical Research: Solid Earth* **116**, (2011).

31. B. A. Black, M. Manga, Volatiles and the tempo of flood basalt magmatism. *Earth and Planetary Science Letters* **458**, 130 (2017).

32. D. Archer, E. Maier-Reimer, Effect of deep-sea sedimentary calcite preservation on atmospheric CO2 concentration. *Nature* **367**, 260 (1994).

33. C. Dessert, B. Dupré, J. Gaillardet, L. M. François, C. J. Allègre, Basalt weathering laws and the impact of basalt weathering on the global carbon cycle. *Chemical Geology* **202**, 257 (2003).

34. C. Dessert, B. Dupré, L. M. François, J. Schott, J. Gaillardet, G. Chakrapani, S. Bajpai, Erosion of Deccan Traps determined by river geochemistry: impact on the global climate and the 87Sr/86Sr ratio of seawater. *Earth and Planetary Science Letters* **188**, 459 (2001/06/15/, 2001).

35. M. J. Henehan, P. M. Hull, D. E. Penman, J. W. Rae, D. N. Schmidt, Biogeochemical significance of pelagic ecosystem function: an end-Cretaceous case study. *Phil. Trans. R. Soc. B* **371**, 20150510 (2016).

36. J. S. Barnet, K. Littler, D. Kroon, M. J. Leng, T. Westerhold, U. Röhl, J. C. Zachos, A new high-resolution chronology for the late Maastrichtian warming event: Establishing robust temporal links with the onset of Deccan volcanism. *Geology* **46**, 147 (2017).

37. T. Westerhold, U. Röhl, B. Donner, H. K. McCarren, J. C. Zachos, A complete high-resolution Paleocene benthic stable isotope record for the central Pacific (ODP Site 1209). *Paleoceanography* **26**, (2011).

38. N. Thibault, D. Husson, Climatic fluctuations and sea-surface water circulation patterns at the end of the Cretaceous era: Calcareous nannofossil evidence. *Palaeogeography, Palaeoclimatology, Palaeoecology* **441**, 152 (2016).

39. M. Mussard, G. Le Hir, F. Fluteau, V. Lefebvre, Y. Goddéris, Modeling the carbon-sulfate interplays in climate changes related to the emplacement of continental flood basalts. *Geological Society of America Special Papers* **505**, (2014).

40. N. Robinson, G. Ravizza, R. Coccioni, B. Peucker-Ehrenbrink, R. Norris, A high-resolution marine 187Os/188Os record for the late Maastrichtian: Distinguishing the chemical fingerprints of Deccan volcanism and the KP impact event. *Earth and Planetary Science Letters* **281**, 159 (2009).

41. G. Ravizza, D. VonderHaar, A geochemical clock in earliest Paleogene pelagic carbonates based on the impact-induced Os isotope excursion at the Cretaceous-Paleogene boundary. *Paleoceanography and Paleoclimatology* **27**, (2012).

42. J. Davies, A. Marzoli, H. Bertrand, N. Youbi, M. Ernesto, U. Schaltegger, End-Triassic mass extinction started by intrusive CAMP activity. *Nature communications* **8**, 15596 (2017).

43. S. D. Burgess, S. A. Bowring, High-precision geochronology confirms voluminous magmatism before, during, and after Earth's most severe extinction. *Science advances* **1**, e1500470 (2015).

44. B. Schoene, J. Guex, A. Bartolini, U. Schaltegger, T. J. Blackburn, Correlating the end-Triassic mass extinction and flood basalt volcanism at the 100,000-year level. *Geology* **38**, 387 (2010).

45. A.-L. Chenet, V. Courtillot, F. Fluteau, M. Gérard, X. Quidelleur, S. F. R. Khadri, K. V. Subbarao, T. Thordarson, Determination of rapid Deccan eruptions across the Cretaceous-Tertiary boundary using paleomagnetic secular variation: 2. Constraints from analysis of eight new sections and synthesis for a 3500-m-thick composite section. *Journal of Geophysical Research* **114**, (2009).

46. L. Li, G. Keller, Abrupt deep-sea warming at the end of the Cretaceous. *Geology* **26**, 995 (1998).

47. N. R. Bondre, R. A. Duraiswami, G. Dole, Morphology and emplacement of flows from the Deccan Volcanic Province, India. *Bulletin of Volcanology* **66**, 29 (2004).

48. P. R. Renne, C. C. Swisher, A. L. Deino, D. B. Karner, T. L. Owens, D. J. DePaolo, Intercalibration of standards, absolute ages and uncertainties in ^{40}Ar/^{39}Ar dating. *Chem. Geol.* **145**, 117 (1998).

49. K. F. Kuiper, A. Deino, F. J. Hilgen, W. Krijgsman, P. R. Renne, J. R. Wijbrans, Synchronizing rocks clocks of Earth history. *Science* **320**, 500 (2008).

50. P. R. Renne, R. Mundil, G. Balco, K. Min, K. R. Ludwig, Joint determination of 40K decay constants and 40Ar/40K for the Fish Canyon sanidine standard, and improved accuracy for 40Ar/39Ar geochronology. *Geochimica et Cosmochimica Acta* **74**, 5349 (2010).

51. C. Hofmann, G. Féraud, V. Courtillot, 40Ar/39Ar dating of mineral separates and whole rocks from the Western Ghats lava pile: further constraints on duration and age of the Deccan traps. *Earth and Planetary Science Letters* **180**, 13 (7/30/, 2000).

52. C. J. Sprain, P. R. Renne, W. A. Clemens, G. P. Wilson, Calibration of chron C29r: New high-precision geochronologic and paleomagnetic constraints from the Hell Creek region, Montana. *Geological Society of America Bulletin*, (2018).

53. S. Khadri, K. Subbarao, J. Walsh, Stratigraphy, form and structure of the east Pune basalts, western Deccan basalt province, India. *MEMOIRS-GEOLOGICAL SOCIETY OF INDIA*, 179 (1999).

54. R. A. Duraiswami, P. Gadpallu, T. N. Shaikh, N. Cardin, Pahoehoe–a′ a transitions in the lava flow fields of the western Deccan Traps, India-implications for emplacement dynamics, flood basalt architecture and volcanic stratigraphy. *Journal of Asian Earth Sciences* **84**, 146 (2014).

55. K. Subbarao, M. Bodas, S. Khadri, J. Beane, Penrose Deccan 2000, Field Excursion Guide to the Western Deccan Basalt Province. *Penrose Field Guides, B. Geological Society of India, ed*, (2000).

56. P. C. Lightfoot, C. J. Hawkesworth, C. W. Devey, N. W. Rogers, P. W. C. V. Calsteren, Source and Differentiation of Deccan Trap Lavas: Implications of Geochemical and Mineral Chemical Variations. *Journal of Petrology* **31**, 1165 (1990).

57. K. G. Cox, C. J. Hawkesworth, Geochemical Stratigraphy of the Deccan Traps at Mahabaleshwar, Western Ghats, India, with Implications for Open System Magmatic Processes. *Journal of Petrology* **26**, 355 (1985).

58. G. Sen, Mineralogy and petrogenesis of the Deccan Trap lava flows around Mahabaleshwar, India. *Journal of Petrology* **27**, 627 (1986).

59. M. R. G. Sayyed, S. M. Hundekari, Preliminary comparison of ancient bole beds and modern soils developed upon the Deccan volcanic basalts around Pune (India): Potential for palaeoenvironmental reconstruction. *Quaternary International* **156-157**, 189 (2006).

60. C. Mitchell, M. Widdowson, A geological map of the southern Deccan Traps, India and its structural implications. *Journal of the Geological Society* **148**, 495 (1991).

61. J. M. Mattinson, Zircon U-Pb chemical-abrasion ("CA-TIMS") method: combined annealing and multi-step dissolution analysis for improved precision and accuracy of zircon ages. *Chem. Geol.* **220**, 47 (2005).

62. N. M. McLean, D. J. Condon, B. Schoene, S. A. Bowring, Evaluating uncertainties in the calibration of isotopic reference materials and multi-element isotopic tracers (EARTHTIME Tracer Calibration Part II). *Geochimica et Cosmochimica Acta* **164**, 481 (2015).

63. D. Condon, B. Schoene, N. McLean, S. Bowring, R. Parrish, Metrology and traceability of U–Pb isotope dilution geochronology (EARTHTIME Tracer Calibration Part I). *Geochimica et Cosmochimica Acta* **164**, 464 (2015).

64. T. E. Krogh, A low contamination method for hydrothermal decomposition of zircon and extraction of U and Pb for isotopic age determination. *Geochim. Cosmochim. Acta* **37**, 485 (1973).

65. A. O. Nier, A redetermination of the relative abundances of the isotopes of carbon, nitrogen, oxygen, argon, and potassium. *Physical Review* **77**, 789 (1950).

66. J. Hiess, D. J. Condon, N. McLean, S. R. Noble, 238U/235U Systematics in Terrestrial Uranium-Bearing Minerals. *Science* **335**, 1610 (2012).

67. U. Schärer, The effect of initial ^{230}Th disequilibrium on young U-Pb ages: the Makalu case, Himalaya. *Earth Planet. Sci. Lett.* **67**, 191 (1984).

68. D. Rubatto, J. Hermann, Experimental zircon/melt and zircon/garnet trace element partitioning and implications for the geochronology of crustal rocks. *Chemical Geology* **241**, 38 (2007).

69. C. B. Keller, B. Schoene, M. Barboni, K. M. Samperton, J. M. Husson, Volcanic–plutonic parity and the differentiation of the continental crust. *Nature* **523**, 301 (2015).

70. J. F. Bowring, N. M. McLean, S. A. Bowring, Engineering cyber infrastructure for U-Pb geochronology: Tripoli and U-Pb_Redux. *Geochem. Geophys. Geosyst.* **12**, Q0AA19 (2011).

71. N. M. McLean, J. F. Bowring, S. A. Bowring, An algorithm for U-Pb isotope dilution data reduction and uncertainty propagation. *Geochem. Geophys. Geosyst.* **12**, Q0AA18 (2011).

72. A. H. Jaffey, K. F. Flynn, L. E. Glendenin, W. C. Bentley, A. M. Essling, Precision measurement of half-lives and specific activities of ^{235}U and ^{238}U. *Phys. Rev.* **C4**, 1889 (1971).

73. B. Schoene, J. L. Crowley, D. C. Condon, M. D. Schmitz, S. A. Bowring, Reassessing the uranium decay constants for geochronology using ID-TIMS U-Pb data. *Geochim. Cosmochim. Acta* **70**, 426 (2006).

74. A. von Quadt, J.-F. Wotzlaw, Y. Buret, S. J. Large, I. Peytcheva, A. Trinquier, High-precision zircon U/Pb geochronology by ID-TIMS using new 10 13 ohm resistors. *Journal of Analytical Atomic Spectrometry* **31**, 658 (2016).

75. B. Schoene, E. F. Baxter, Petrochronology and TIMS. *Reviews in Mineralogy and Geochemistry* **83**, 231 (2017).

76. J. S. Miller, J. P. Matzel, C. F. Miller, S. D. Burgess, R. B. Miller, Zircon growth and recycling during the assembly of large, composite arc plutons. *Jour. Vol. Geotherm. Res.* **167**, 282 (2007).

77. A. K. Schmitt, D. F. Stockli, J. M. Lindsay, R. Robertson, O. M. Lovera, R. Kislitsyn, Episodic growth and homogenization of plutonic roots in arc volcanoes from combined U-Th and (U-Th)/He zircon dating. *Earth and Planetary Science Letters* **295**, 91 (2010).

78. C. R. Bacon, J. B. Lowenstern, Late Pleistocene granodiorite source for recycled zircon and phenocrysts in rhyodacite lava at Crater Lake, Oregon. *Earth and Planetary Science Letters* **233**, 277 (2005).

79. J. Ramezani, M. D. Schmitz, V. I. Davydov, S. A. Bowring, W. S. Snyder, C. J. Northrup, High-precision U-Pb zircon age constraints on the Carboniferous-Permian boundary in the southern Urals stratotype. *Earth Planet. Sci. Lett.* **256**, 244 (2007).

80. V. I. Davydov, J. L. Crowley, M. D. Schmitz, V. I. Poletaev, High-precision U-Pb zircon age calibration of the global Carboniferous time scale and Milankovitch band cyclicity in the Donets Basin, eastern Ukraine. *Geochem. Geophys. Geosyst.* **11**, Q0AA04 (2010).

81. J.-F. Wotzlaw, S. K. Hüsing, F. J. Hilgen, U. Schaltegger, High-precision zircon U–Pb geochronology of astronomically dated volcanic ash beds from the Mediterranean Miocene. *Earth and Planetary Science Letters* **407**, 19 (2014).

82. J.-F. Wotzlaw, J. Guex, A. Bartolini, Y. Gallet, L. Krystyn, C. A. McRoberts, D. Taylor, B. Schoene, U. Schaltegger, Towards accurate numerical calibration of the Late Triassic: High-precision U-Pb geochronology constraints on the duration of the Rhaetian. *Geology* **42**, 571 (2014).

83. S. D. Burgess, S. Bowring, S.-z. Shen, High-precision timeline for Earth's most severe extinction. *Proceedings of the National Academy of Sciences* **111**, 3316 (2014).

84. D. J. Lehrmann, J. Ramezani, S. A. Bowring, M. W. Martin, P. Montgomery, P. Enos, J. L. Payne, M. J. Orchard, W. Hongmei, W. Jiayong, Timing of recovery from the end-Permian extinction: Geochronologic and biostratigraphic constraints from south China. *Geology* **34**, 1053 (2006).

85. B. B. Sageman, B. S. Singer, S. R. Meyers, S. E. Siewert, I. Walaszczyk, D. J. Condon, B. R. Jicha, J. D. Obradovich, D. A. Sawyer, Integrating 40Ar/39Ar, U-Pb, and astronomical clocks in the Cretaceous Niobrara Formation, Western Interior Basin, USA. *Geological Society of America Bulletin*, (2014).

86. N. Metropolis, A. W. Rosenbluth, M. N. Rosenbluth, A. H. Teller, E. Teller, Equation of state calculations by fast computing machines. *The journal of chemical physics* **21**, 1087 (1953).

87. E. B. Watson, Dissolution, growth and survival of zircons during crustal fusion: kinetic principals, geological models and implications for isotopic inheritance. *Earth and Environmental Science Transactions of the Royal Society of Edinburgh* **87**, 43 (1996).

88. K. M. Samperton, E. A. Bell, M. Barboni, C. B. Keller, B. Schoene, Zircon age-temperature-compositional spectra in plutonic rocks. *Geology* **45**, 983 (2017).

89. J. Guex, B. Schoene, A. Bartolini, J. Spangenberg, U. Schaltegger, L. O'Dogherty, D. Taylor, H. Bucher, V. Atudorei, Geochronological constraints on post-extinction recovery of the ammonoids and carbon cycle perturbations during the Early Jurassic. *Palaeogeography, Palaeoclimatology, Palaeoecology* **346-347**, 1 (2012).

90. S. R. Meyers, S. E. Siewert, B. S. Singer, B. B. Sageman, D. J. Condon, J. D. Obradovich, B. R. Jicha, D. A. Sawyer, Intercalibration of radioisotopic and astrochronologic time scales for the Cenomanian-Turonian boundary interval, Western Interior Basin, USA. *Geology* **40**, 7 (2012).

91. J. Haslett, A. Parnell, A simple monotone process with application to radiocarbon-dated depth chronologies. *Journal of the Royal Statistical Society: Series C (Applied Statistics)* **57**, 399 (2008).

92. D. De Vleeschouwer, A. C. Parnell, Reducing time-scale uncertainty for the Devonian by integrating astrochronology and Bayesian statistics. *Geology* **42**, 491 (2014).

93. F. M. Gradstein, G. Ogg, M. Schmitz, *The Geologic Time Scale 2012 2-Volume Set*. (elsevier, 2012).

94. P. R. Renne, I. Arenillas, J. A. Arz, V. Vajda, V. Gilabert, H. D. Bermúdez, Multi-proxy record of the Chicxulub impact at the Cretaceous-Paleogene boundary from Gorgonilla Island, Colombia. *Geology* **46**, 547 (2018).

95. C. J. Sprain, P. R. Renne, G. P. Wilson, W. A. Clemens, High-resolution chronostratigraphy of the terrestrial Cretaceous-Paleogene transition and recovery interval in the Hell Creek region, Montana. *Bulletin* **127**, 393 (2015).

96. J.-F. Wotzlaw, U. Schaltegger, D. A. Frick, M. A. Dungan, A. Gerdes, D. Günther, Tracking the evolution of large-volume silicic magma reservoirs from assembly to supereruption. *Geology* **41**, 867 (2013).

97. K. Min, R. Mundil, P. R. Renne, K. R. Ludwig, A test for systematic errors in $^{40}Ar/^{39}Ar$ geochronology through comparison with U-Pb analysis of a 1.1 Ga rhyolite. *Geochim. Cosmochim. Acta* **64**, 73 (2000).

98. J. Laskar, A. Fienga, M. Gastineau, H. Manche, La2010: a new orbital solution for the long-term motion of the Earth. *Astronomy & Astrophysics* **532**, A89 (2011).

99. T. Westerhold, U. Röhl, I. Raffi, E. Fornaciari, S. Monechi, V. Reale, J. Bowles, H. F. Evans, Astronomical calibration of the Paleocene time. *Palaeogeography, Palaeoclimatology, Palaeoecology* **257**, 377 (2008).

100. M. Sinnesael, D. De Vleeschouwer, R. Coccioni, P. Claeys, F. Frontalini, L. Jovane, J. F. Savian, A. Montanari, High-resolution multiproxy cyclostratigraphic analysis of environmental and climatic events across the Cretaceous-Paleogene boundary in the classic pelagic succession of Gubbio (Italy). *The Stratigraphic Record of Gubbio: Integrated Stratigraphy of the Late Cretaceous–Paleogene*

Umbria-Marche Pelagic Basin, edited by: Menichetti, M., Coccioni, R., and Montanari, A., Geological Society of America Special Paper **524**, 115 (2016).

101. D. Husson, B. Galbrun, J. Laskar, L. A. Hinnov, N. Thibault, S. Gardin, R. E. Locklair, Astronomical calibration of the Maastrichtian (Late Cretaceous). *Earth and Planetary Science Letters* **305**, 328 (2011).

102. D. Husson, B. Galbrun, S. Gardin, N. Thibault, Tempo and duration of short-term environmental perturbations across the Cretaceous-Paleogene boundary. *Stratigraphy* **11**, 159 (2014).

103. S. J. Batenburg, A. S. Gale, M. Sprovieri, F. J. Hilgen, N. Thibault, M. Boussaha, X. Orue-Etxebarria, An astronomical time scale for the Maastrichtian based on the Zumaia and Sopelana sections (Basque country, northern Spain). *Journal of the Geological Society* **171**, 165 (2014).

104. S. J. Batenburg, M. Sprovieri, A. S. Gale, F. J. Hilgen, S. Hüsing, J. Laskar, D. Liebrand, F. Lirer, X. Orue-Etxebarria, N. Pelosi, Cyclostratigraphy and astronomical tuning of the Late Maastrichtian at Zumaia (Basque country, Northern Spain). *Earth and Planetary Science Letters* **359**, 264 (2012).

105. F. J. Hilgen, K. F. Kuiper, L. J. Lourens, Evaluation of the astronomical time scale for the Paleocene and earliest Eocene. *Earth and Planetary Science Letters* **300**, 139 (2010).

106. E. Thomas, E. Barrera, N. Hamilton, B. Huber, J. Kennett, S. O'Connell, J. Pospichal, V. Spiefl, L. Stott, W. Wei, Upper Cretaceous-Paleogene Stratigraphy of sites 689 and 690, Maud Rise (Antarctica) (1990).

Acknowledgements

This paper benefited from comments made by three anonymous reviewers and discussions with A. Maloof and J. Higgins. Field assistance was provided by M. Coronado, P. Kemeny, and V. Sordet. J. Punekar provided critical field assistance and sample recollection. A. Chen, S. Gwizd, A. Hager, and D. Okhai are also thanked for tirelessly separating zircons from redbole samples. **Funding:** Field and labwork was supported by NSF grant EAR-1454430 to Schoene and G. Keller and by the Princeton

Dept. of Geosciences Scott Fund. Lawrence Livermore National Laboratory is operated by Lawrence Livermore National Security, LLC, for the U.S. Department of Energy, National Nuclear Security Administration under Contract DE-AC52-07NA27344. LLNL contribution LLNL-JRNL-755419. **Author contributions**: All authors except CBK participated in fieldwork and sample collection; U-Pb geochronology was done by KMS, MPE and BS; Bayesian Modeling was done by CBK, KMS and BS; Manuscript and figures were prepared by BS, MPE and KMS with input from GK, TA, CBK, and SFRK. **Competing interests:** the authors have no competing interests to declare. **Data and Materials availability**: All methods, data, and codes used for modeling are available in the manuscript or supplementary material.

Figures:

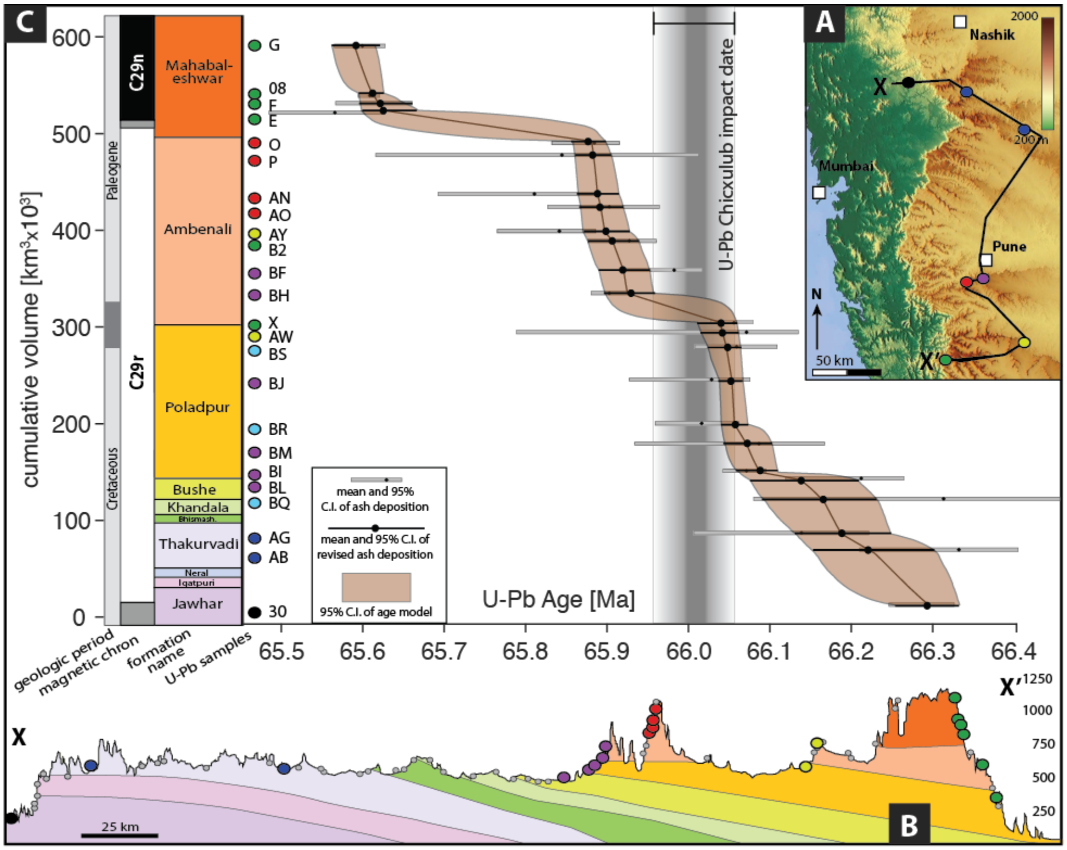

Figure 1: Stratigraphy, sampling transects, and U-Pb age model for the Deccan Traps. (A) Elevation map of study location in the Western Ghats, India. Cross section X-X' shown by black segmented line. Sampling transects located by colored dots. (B) Geologic cross-section through the field area, with sample locations indicated. Different basalt formations in the Deccan Traps color-coded to stratigraphic column in C. Cross-section based on previous work (*14-17*), modified based our geochronology. (C) Volumetric stratigraphic column and magnetic chrons of the major formations of the Deccan Traps (*22, 45*), shown as hundreds of thousands of km^3. Sample heights plotted ("RB" sample prefix omitted), based on composite stratigraphic section compiled in Fig. S2. Age model for the Deccan Traps based on our U-Pb geochronology shown with 95% credible intervals. Horizontal gray bars indicate eruption ages derived from populations of zircon dates from each horizon, and black horizontal bars show dates refined from the stratigraphic Bayesian model. Vertical gray-shaded bar shows an age for the Chicxulub impact (*25*).

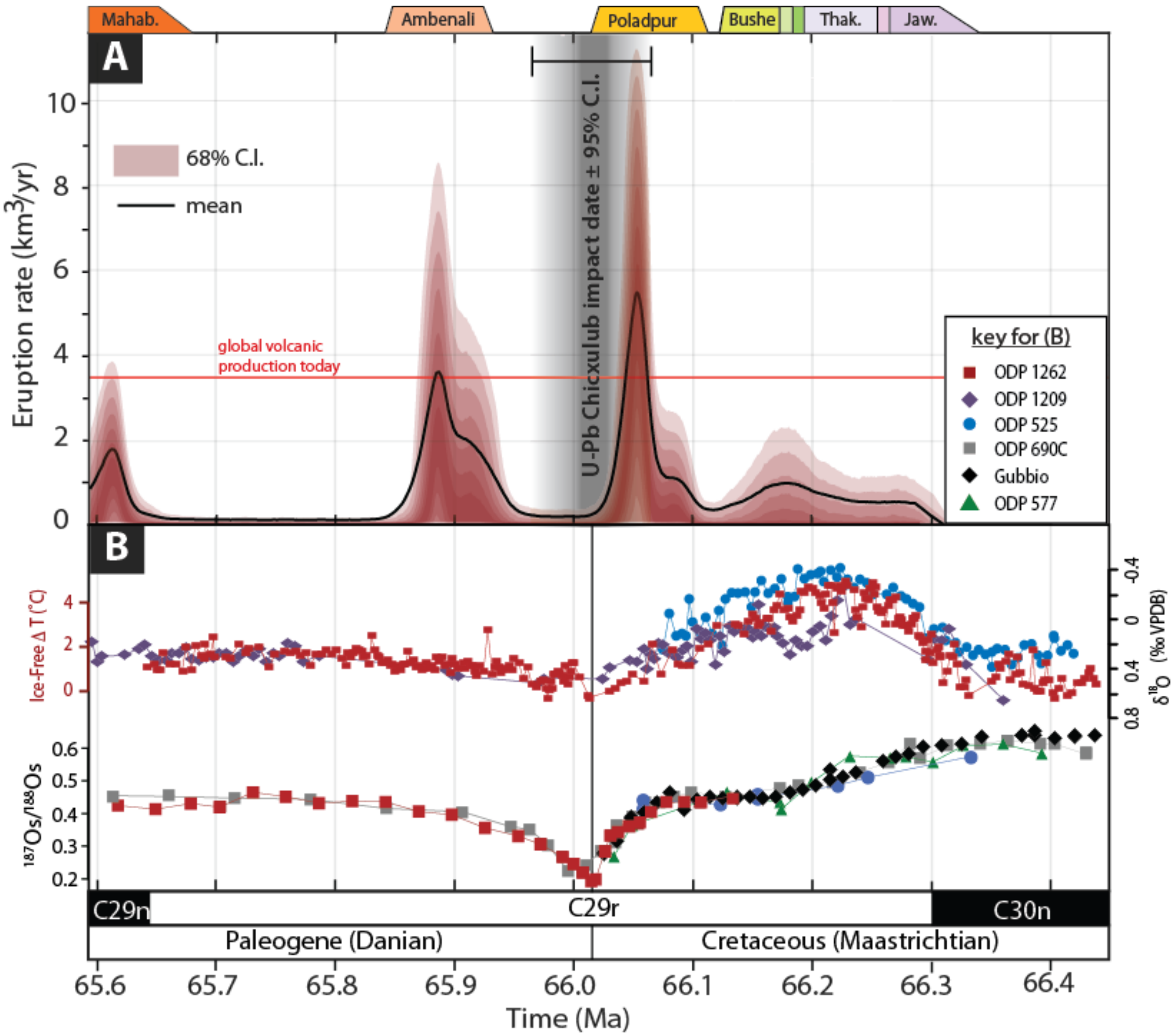

Figure 2: Eruption rate model for the Deccan Traps, based on U-Pb geochronology. (A) Results from the MCMC algorithm used to generate the age model in Fig. 1, converted to a probabilistic volumetric eruption rate for the Deccan Traps shown with contours up to 68% credible intervals. U-Pb date for the Chicxulub impact same as Fig. 1. Total global volcanic productivity (~3-4 km³/yr) includes mid ocean ridges and volcanic arcs (*28*). (B) Compilation of proxy records from ODP cores and outcrops. Top shows $\delta^{18}O$ of species-specific benthic foraminifera from ODP 525 (*46*), ODP 1262 (*36*), and ODP 1209 (*37*). Temperature calculated for benthic foraminifera *N. Truempyi* in ODP 1262 (*36*). Osmium isotopic records come from bulk carbonate from both ODP cores and outcrop (*40, 41*). Age models are described in Supp. Materials (*13*).